Two-dimensional spectroscopic time series of solar granulation

Hanslmeier Arnold
Institut für Geophysik, Astrophysik und Meteorologie, Univ.-Platz 5, A-8010 Graz, Austria

Kučera Ales, Rybák Jan
Astronomical Institute, Slovak Academy of Sciences, SK-05960 Tatranská Lomnica, Slovakia

Wöhl Hubertus
Kiepenheuer-Institut für Sonnenphysik, Schöneckstr. 6, D-79104 Freiburg, Germany

Sep 11, 2003

Abstract. In this paper we investigate the dynamics of the solar granulation by analyzing time series of 2D spatially highly resolved spectrograms. These were obtained by spatial scans covering a field of $12.8'' \times 20''$. The advantage of this method is a high spectral resolution however the data are not taken simultaneously and to cover the field described above 50 exposures taken sequentially in time are necessary. Therefore, to obtain one map about 2 minutes are required.

Plots of the evolution of different line parameters are given as well as the decay of correlation functions. The correlations between the first map of line parameters and successive maps (which are separated by about 2 minutes) were investigated showing a rapid decay down to correlation coefficient of 0.4 within 4 minutes, the velocity pattern in the field observed varies on smaller time scales. The temporal variation of correlation between the line parameters for the different lines shows a periodic signal related to 5 min oscillations which could not be totally filtered. The evolution of the correlation functions between line parameters is analyzed which gives an error estimate of all correlation values found in the literature.

For the first time it is explicitly shown how evolution in a selected photospheric fields influences on the evolution of granular/intergranular structures.

Keywords: Sun: granulation – Sun: photosphere

1. Introduction

The solar photosphere is a highly dynamic and rather rapidly evolving layer. The dynamics of convective motions at small scales in the photosphere can be divided roughly into upward streaming plasma (granulum) and downward streaming plasma (intergranulum). Recent reviews about solar granulation were given by Muller (1999) and Hanslmeier (2003) and more citations can be found therein.

From the observational point of view there are two ways to study these motions. *Spectroscopic observations* give information about Doppler velocities, line broadening etc. Line profiles from granular and intergranular regions are different, the bisectors vary from granulum to intergranulum (Wiehr and Kneer (1988), Holweger & Kneer (1989), Lites et al. (1989), Hanslmeier et al. (1993)). Enhanced line broadening in the intergranular space can be interpreted as a manifestation of enhanced turbulence. In Nesis et al. (1992, 1993) and Hanslmeier et al. (1993, 1994) line profiles from individual granules are analyzed. Komm et al. (1990, 1991a, 1991b) followed the dynamics in different height levels by deriving the line parameters at different line depths and using lines of different formation heights.

In order to study the dynamics of these motions, time series are required.

Using a 16 min time series of two-dimensional "Multichannel Subtractive Double Pass" spectrograms, recorded in the Na D_2 5690 Å line Espagnet et al. (1995) studied the propagation of temperature and velocity fields as a function of height in the photosphere. They found that above 60 to 90 km over the continuum level the intensity features are not related to the granules. The velocity fluctuations associated to the granulation cross the whole thickness of the photosphere. The photosphere can thus be separated into two distinct layers.

Kučera et al. (1995) studied Fe I lines in the quiet photosphere in purely quiet regions and moderate active regions.

Krieg et al. (1999, 2000) investigated granular velocities and their relation to the granular intensity pattern from the disc center of the Sun using speckle methods to two-dimensional narrow-band images in Na D_2 from the "Göttingen" Fabry- Perot interferometer (FPI). They found high small scaled velocity and upflows that coincide frequently with the bright borders of granules or with small-scale brightenings. While the intensity pattern exhibits a clearly non-Gaussian distribution, the velocity distribution can be represented by a Gaussian with a "macroturbulent" velocity of 0.825 kms^{-1}. Hirzberger et al. (2001) studied time series of spectral scans across the non magnetic Fe 5576Å line at the disk center. These 2-D spectroscopic images were then reconstructed with speckle methods and a spatial resolution about 0.4 $''$ was achieved.

Another possibility to study the evolution of solar granulation is to analyze *time series of images*. Hirzberger et al. (1997) used a 90 minute time series of high resolution solar white light images to derive information on the growth and decay of granulation. With a tunable filter to scan an image through the line profile (Göttingen FPI, Bendlin and Volkmer, 1995), TESOS (Telecentric Etalon SOlar Spectrometer, Kentischer et al., 1998) information on the line parameters at different heights in the line forming region can be obtained. Bellot Rubio et al (2003) used the TESOS system (resolution 250000) to construct maps of various spectroscopic parameters and computed the line asymmetries induced by the Evershed flows investigated by means of a bisector analysis of the FeI line at 5576 Å.

A great number of theoretical papers on the dynamics can be found in the literature. A recent review focussed on theoretical aspects was given by Nordlund (2003).

Apslund et al. (2000) used ab-initio 3-D, radiative-hydrodynamical convection simulations of the solar granulation to simulate Fe I and Fe II line formation. The non-thermal line broadening is mainly provided by the Doppler shifts arising from the convective flows in the solar photosphere and from the solar oscillations. Frutiger et al. (2000) applied inversion techniques to derive properties of stellar and solar granulation using spectra of photospheric lines at the disk center and integrated over the whole disk.

In the papers of Gadun et al. (1997, 1999) theoretical spectral scans were used to reproduce and interpret correlative relationships derived from spectral observations. Hanslmeier et al. (2000) investigated the behavior of the higher photosphere. In the paper of Gadun et al. (2000) correlative height-dependent relationships between selected quantities of 2-D model atmospheres are investigated. These theoretical correlations are derived directly from time-dependent 2-D models.

In this paper we try to analyze granular/intergranular characteristics using the latter technique. We obtained a similar spatial resolution (0.4 ″) as with FPI data. The advantage of the scanning method is that the further reduction procedures are much easier and also the spectral resolution is higher. From the line profiles the line parameters were determined. These parameters are related to physical properties of the solar atmosphere. Moreover, by using time series, we can follow their temporal evolution.

It is evident that such a study can only be done with a compromise: the seeing changes during the observations and therefore only short time periods can be selected from the whole data set that are homogeneous enough to follow the evolution.

2. Observations and Data Reduction

The data were taken with the 70 cm Vacuum Tower Telescope at the Observatorio del Teide in Izaña, Tenerife, on June 2, 1999. A more detailed description of this telescope can be found in Schröter et al. (1985).

We obtained during the observing campaign two dimensional "images" of the line parameters by scanning over the solar surface, where the spatial sampling interval was $0.4''$ and the total number of slit positions was 50. The slit length was $12.8''$ covered by 100 individual spectral rows and therefore a total area of $12.8''$ x $20''$ was scanned. Thus the resolution of the original data was $0.128''$ in the y direction and $0.4''$ in the x direction. In order to obtain similar step widths in the x- and y- direction, a resampling of the data was applied.

The time step between two successive slit positions was $2.5\,s$. Thus one 2-D scan lasted 125 s, data storage required another 5 s. Seven 2-D images were obtained in total. The exposure time of the images was 20 ms. The slit width 120μm. The spectrograms contained the two lines:

- Line I: Fe I at 630.1508 nm of $W_\lambda = 127\,$mÅ, $EP = 3.64\,$eV and $g_{\rm eff} = 1.6$, estimated line core formation height 378 km (Gadun et al., 2000),
- Line II: Fe I at 630.2499 nm of $W_\lambda = 83\,$mÅ, $EP = 3.69\,$eV and $g_{\rm eff} = 2.5$, estimated line core formation height 270 km (Gadun et al., 2000).

From these data the following parameters were calculated after applying the usual (dark current, flat field) and some special image reduction procedures (that were necessary because of slight differences between flat fields and images; this is called camera flat field and telescope flat field, for details please refer to Wöhl et al., 2002): continuum intensity $I_{\rm c}$, line center residual intensity $I_{\rm r}$, line center Doppler velocity $v_{\rm c}$, full width at half maximum $f_{\rm w}$.

The continuum intensity $I_{\rm c}$ was taken at the left and right side of the line in the undisturbed continuum respective to the line center. Doppler velocities were measured by fitting the line center and extracting the minimum position. All Doppler velocity values were averaged and the particular value of the velocity for a particular time and position was calculated as a difference from the average values (blueshift negative values, dark in the maps; redshift positive values, bright in the maps).

In the next paragraph seven 2-D maps of the spectral characteristics each separated by 125 s are analyzed in order to follow the evolution of the solar photospheric fine structures reflected in the spectral characteristics.

We observed in the disk center in a quiet solar region (this was checked by simultaneously taken Hα images). Since we wanted to observe quiet solar granulation the usage of the VTT correlation tracker was not possible because it works only for objects of higher contrast (e.g. small pores) and problems with the scanning would have occurred. The sky transparency was constant during the observing period.

In order to minimize influences due to non convective oscillatory motions and effects of seeing between the scans and 2-D maps, the data were filtered in the following way. Each scan was filtered for scales $> 3.6''$ and for scales at noise level ($< 0.4''$). Such a filter was already proposed by Mattig and Schlebbe (1974) and applied to study granular velocities separated from oscillatory components (see also Hanslmeier et al., 1990). Of course the seeing influences the data and therefore a noise level at $0.4''$ was assumed moreover that value arises from the scanning stepwidth described above.

3. Results

In the following panels we give the variation of the above mentioned line parameters as a function of time (in the vertical direction, the first 2-D map at the bottom, the last of the sequence at the top) by 2-D maps. The horizontal direction is the normal to the slit.

3.1. Global relationships

Fig. 1 shows the variation of continuum intensity $I_{\rm c}$ for line I (1st column) and for line II (2nd column) and residual intensity $I_{\rm r}$ for line I (3rd column) and line II (4th column) in 7 separate maps as a function of time (in the vertical direction). Fig. 2 gives the data for the full width at half maximum $f_{\rm w}$ (line I, 1st column, line II, 2nd column) and velocity $v_{\rm c}$ (line I, 3rd column, line II, 4th column).

It is clear that in Fig. 1 the first two columns must be nearly identical since the continuum is taken near both lines which are only separated by 0.2 nm. But this also serves as a test whether the continuum has been chosen appropriately. Due to the filtering, noise induced by seeing is reduced.

In Table I the maximum and minimum values of the parameters plotted are given.

By comparing these two figures we can see the following trends:

- In the first two columns of Fig. 1 the intensity pattern is typical for granular/intergranular structure.

- The $I_{\rm r}$ maps in columns 3 and 4 of Fig. 1 are quite similar for the two lines which have a different line formation height. This indicates that the temperature fields are similar at these heights if the intensity fluctuations can be attributed purely to temperature fluctuations (neglecting possible pressure variations). Also clearly the evolution of this temperature field is seen when following from the bottom to the top the individual 2-D maps in column 3 and 4 of Fig. 1.

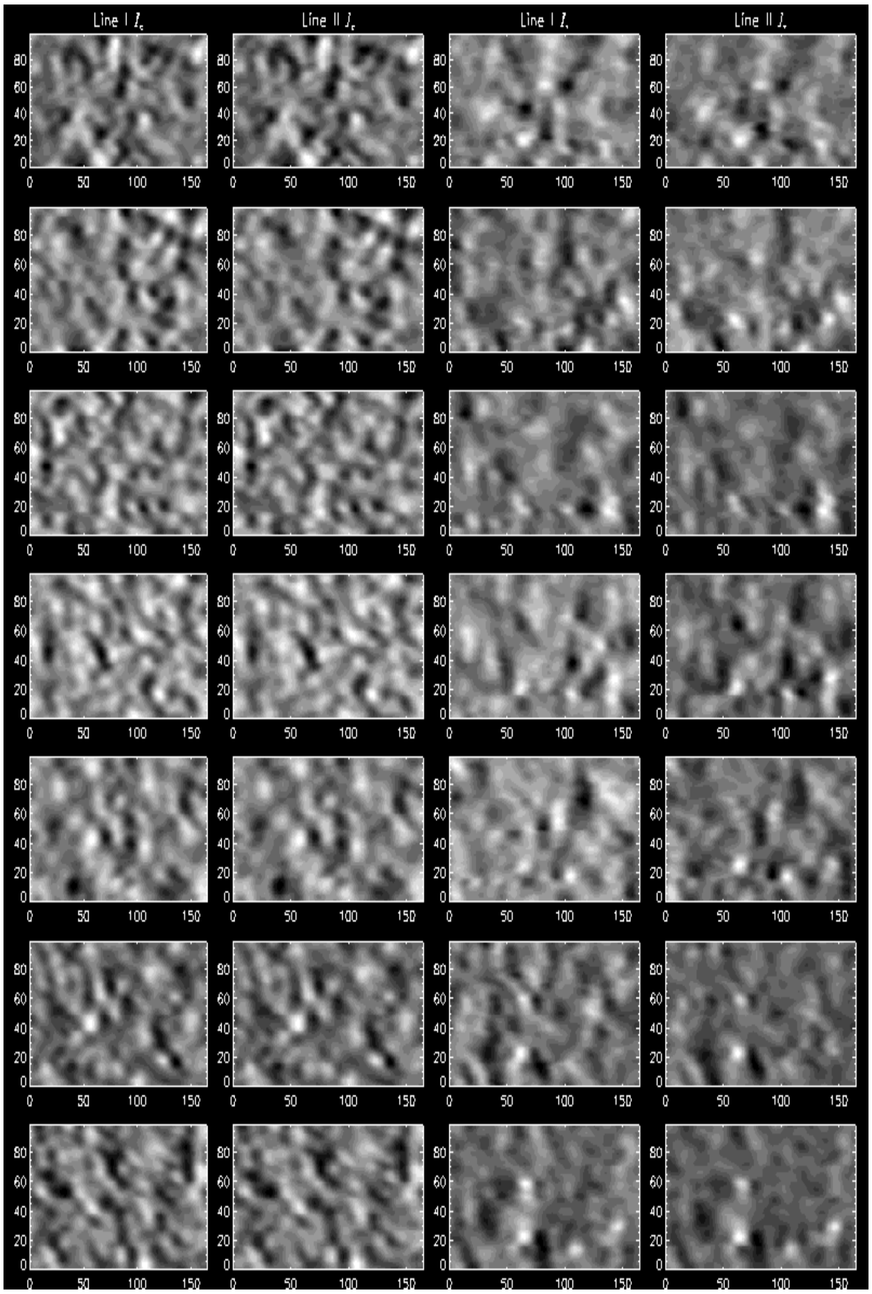

Figure 1. Temporal evolution (vertical, from bottom to the top) of continuum intensity I_{c} for lines I, and II (1st and 2nd columns from the left) and residual intensity I_{r} for lines I and II (3rd and 4th columns from the left). Higher (lower) intensities are coded white (black). In each 2-D map the range on the x-axis is $20''$ and on the y-axis $12.8''$. The time step between the 2-D maps is 125 s.

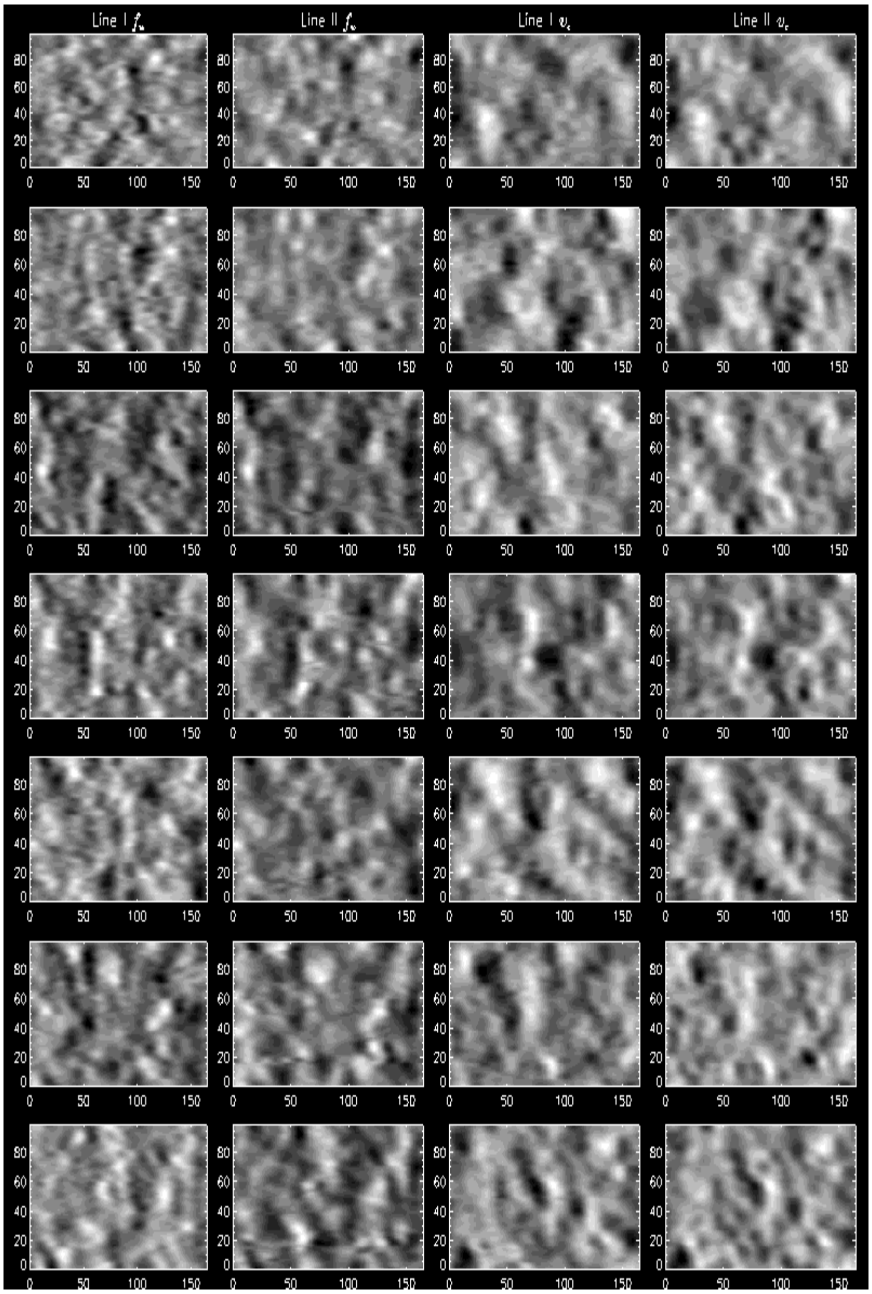

Figure 2. Temporal evolution (vertical, from bottom to the top) of full width at half maximum f_w for lines I, and II (1st and 2nd columns from the left) and line center velocities v_c for lines I and II (3rd and 4th columns from the left). Higher (lower) values are coded white (black). In each 2-D map the range on the x-axis is $20''$ and on the y-axis $12.8''$.The time step between the 2-D maps is 125 s.

Table I. Maximum and minimum values of the line parameters plotted in Figs. 1 and 2. in % of the mean values.

Line	Parameter	Max.	Min.
Line I	I_{c}	115	84
	I_{r}	139	71
	f_{w}	117	89
	v_{c}	658 m/s	-846 m/s
Line II	I_{c}	116	84
	I_{r}	143	77
	f_{w}	121	88
	v_{c}	564 m/s	-705 m/s

- Maxima and minima of I_{r} fluctuations which are nearly identical for the two different lines (columns 3 and 4 of Fig. 1).
- No correlation between maxima and minima of the I_{r} maps with the I_{c} maps can be seen. There seem to be regions with an anticorrelation, where minima of I_{c} coincide with maxima in the I_{r} maps.
- The evolution of the line center velocity fluctuations for the two different lines is similar however there seems to be no correlation of the structures with the intensity fluctuations I_{r} and I_{c} (compare Fig. 1, columns 1 and 2 and Fig. 2, columns 3 for line I and 4 for line II). Some features seen in the panels of v_{c} fluctuations can be recognized in the corresponding residual intensity fluctuations thus the correlations is slightly higher.
- The evolution for the f_{w} variations is quite similar for the two different lines.

3.2. Correlations

In this section we give the results of a correlation analysis. In the following figures the full line denotes the correlation for line I and the dotted line for the line II which has a deeper formation height. The correlations were calculated for the whole 2D map. The correlations were calculated in the following way:

Autocorrelation: the first 2-D map of the time sequence ($i = 0$) was correlated with all subsequent 2-D maps ($0 \leq i \leq 6$) thus an evolution should be noticed by a decrease of the autocorrelation with time due to the physical evolution of the plasma in the observed region. In Fig. 3 the autocorrelation is shown for the 4 line parameters. In order to have estimates on the variation of these correlations within the maps we give in Fig. 3 error bars resulting from the variation of the correlation coefficients in the different rows of the respective maps. These error bars result from variations due to different granular/intergranular sampling and evolution as well as seeing variations between the scans. Since the extension of the field is relatively small the granular evolution dominates the error bars.

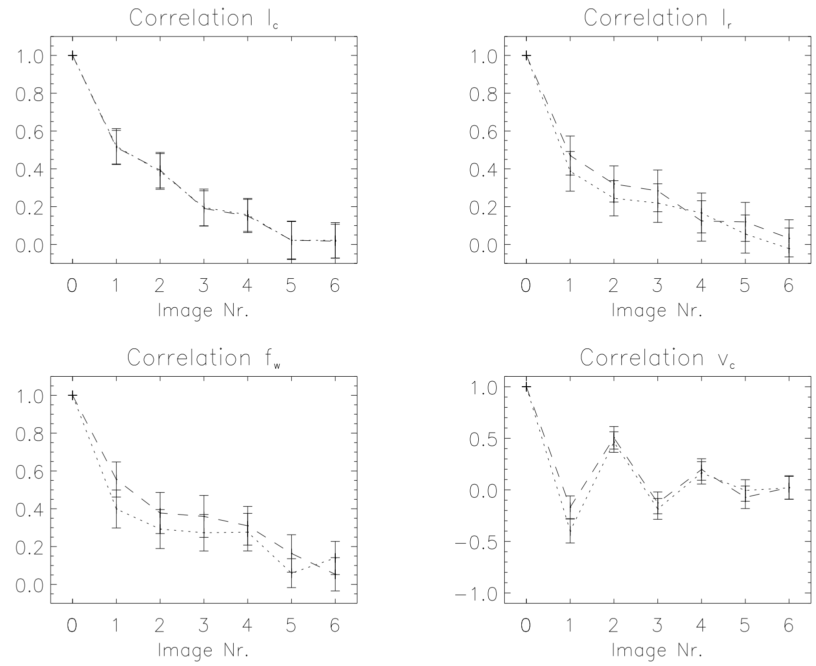

Figure 3. Temporal variation of the correlation coefficients for different line parameters. The 2-D map at $i = 0$ was correlated with the 2-D maps at $0 \leq i \leq 6$. In the case of line II (dashed) the correlation values are slightly higher.

For the line parameters I_c, I_r and f_w the behavior is very similar: the correlation between the first map of the line parameter and the second falls down to 0.4 and then decreases with a smaller gradient. For the deeper originating line II (dashed line) the correlation is slightly higher. The correlation of the first map of v_c with the other maps oscillates between positive and negative values and is very similar for both lines. The v_c autocorrelation coefficient goes to zero as a damping wave.

Let us now study the cross correlations between pairs of line parameters and their temporal variation. (Fig. 4). Here, the crosscorrelations were calculated for the line parameters for pairs of 2-D maps at the same time t_i, $0 \leq i \leq 6$.

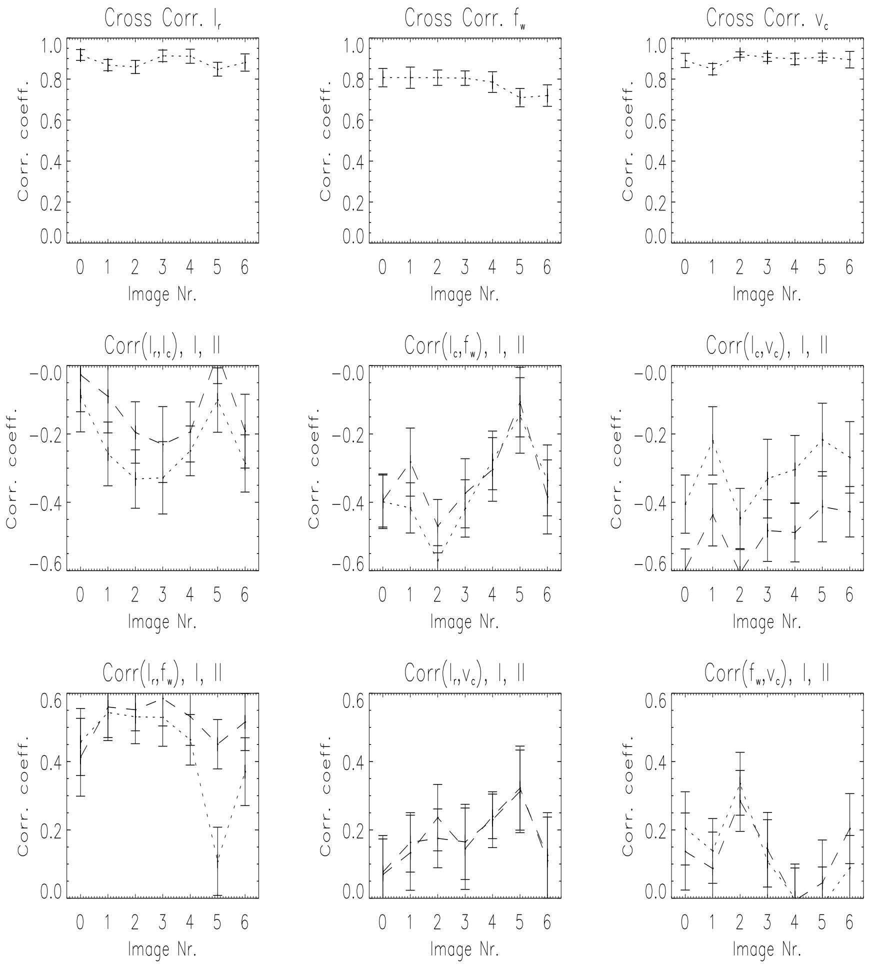

Figure 4. Temporal variation of the crosscorrelation coefficients for different line parameters. Dotted: line I, dashed: line II

- In the first row of Fig. 4 the variation of the crosscorrelation of the line parameters for line I and line II as a function of time is shown for the line parameters residual intensity, full width at half maximum and line center velocity. The correlation coefficients are above 0.8 and show some variations which can be mainly attributed to the evolution within the field investigated. The correlations are largest for the velocities (correlation above 0.9 during the time series) and lowest for the f_{w} (correlation about or below 0.8 during the time series).

- corr($I_{\mathrm{c}}, I_{\mathrm{r}}$): there is only a weak crosscorrelation which varies with time for all 2-D maps in the sequence. The maximum values are -0.35.
- corr($I_{\mathrm{c}}, f_{\mathrm{w}}$): here the strongest correlation occurred but it also varies with time. The maximum value was -0.6. The correlation was found somewhat lower for the deeper line.
- corr($I_{\mathrm{c}}, v_{\mathrm{c}}$): this again strongly oscillates, there was a maximum negative value of -0.45 for line I and -0.55 for line II.
- corr($I_{\mathrm{r}}, f_{\mathrm{w}}$): the correlation remained relatively stable for the first 10 minutes near 0.5 then decreases.
- corr($I_{\mathrm{r}}, v_{\mathrm{c}}$) oscillates and has a maximum near the end of the time series.
- corr($f_{\mathrm{w}}, v_{\mathrm{c}}$): remains below 0.3 and oscillates.
- The error bars given are explained in the previous section. They mainly result from the influence of granular evolution.

In the panels of Fig. 1 and 2 we can also follow the evolution of individual structures. This will be discussed in more detail in a further paper.

3.3. Influence of seeing

The data were not corrected for any seeing influence. Therefore, it is extremely important to give an objective estimate of seeing influences on the data which can lead to distortion in the 2-D maps of the time series of the line parameters.

In Fig. 5 we show the standard deviation of the I_{c} values over each of the I_{c} maps. The values were calculated for each exposure and then averaged over one 2-D map. It is seen that this parameter slowly declines from 5% to 4%. For a comparison the variation is also given for the unfiltered data (which are not shown in the other figures of the paper) in order to demonstrate the influence of the filter by reducing small scale fluctuations contributing to I_{c} fluctuations.

In Figures 6 the variation of the correlation between successive images is shown for the different line parameters. Thus the correlation

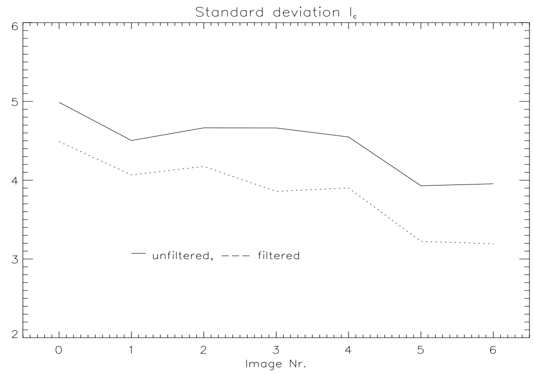

Figure 5. Variation of the standard deviation of I_c as a function of time.

coefficient between e.g. the image #0 and image #1 in the time series for the continuum intensity is slightly less than 0.6. It is clearly seen that there is still a variation due to oscillations which of course can be only filtered out appropriately when having a 2-D long lasting time series using a mask in the $k - \omega$ diagram. The values are larger for line 2 in the case of residual intensity and full width at half maximum variations and are lower for line 2 in the case of line center velocity fluctuations.

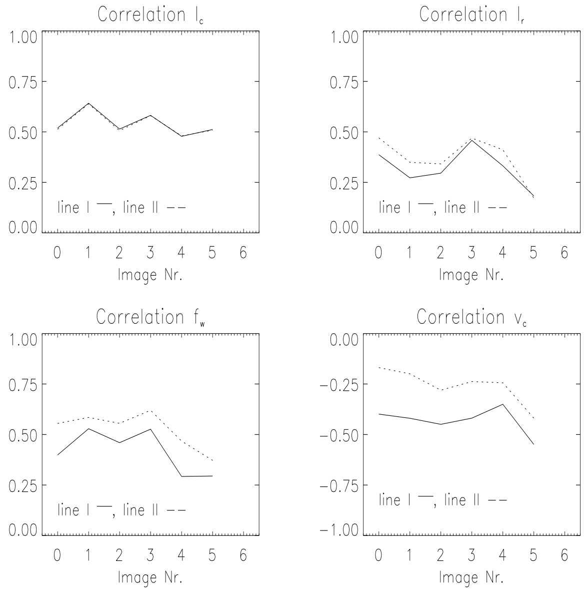

Figure 6. Variation of the correlation coefficient between successive images for the four different line parameters.

It is shown, that the filtering more effectively works on the velocity fluctuations as it has to be expected.

It is seen from these figures that the correlation coefficients remain similar. If there would be strong seeing influences than the fluctuations should be larger. The fluctuations as they are observed can be explained by fluctuations due to the evolution in the relatively small field considered.

4. Discussion

We have studied the evolution of different lines parameters from two dimensional scans over a period of approximately 14 minutes.

As it has been stated previously, the difference in line core formation height between the two lines studied here is about 100 km. Therefore, using Doppler velocities v_{c} and residual intensities I_{r} we follow the radial motions and temperature fluctuations in two different levels. The continuum intensities I_{c} derived for both lines provide information on temperature fluctuations in the same level at the bottom of the photosphere.

The full width at half maximum fluctuations of both lines should reflect physical conditions between the continuum level and the lower level. The difference in height between these two layers should be negligible due to the broad profiles of the response functions.

The deeper formed line II has a larger g_{eff} thus the influence of magnetic elements should be larger in the f_{w} of this line.

Temperature fields

The variation of temperature fields can be estimated from the variation of the continuum intensity fluctuations I_{c} and line center residual intensity fluctuations I_{r}. The visual inspection of the maps of time series (Fig. 1) shows that the I_{c} maps reveal more fine structures than the I_{r} maps. This is also reflected by the decay of the correlation between the first map of the time series and the subsequent maps. The decay seems to be stronger for the I_{r} maps which can be seen by the steeper decline of the correlation. For line II the I_{r} decay is more like the I_{c} decay. The behavior of the correlation between successive maps (see Fig. 6) also shows that in the case of I_{c} the values fluctuate about 0.6 and in the case of I_{r} the fluctuations are about 0.5 and for the line II they are again higher.

Fig. 4 shows that there is a very weak correlation between the temperature fields at continuum and line core formation height and that the values strongly oscillate with time but are below -0.35. Thus temperature fields are not coherent between these heights and decay. The correlation is strongly time dependent and of course influenced by the evolution in the field.

Coupling between velocity and temperature fields

The decay of the correlation of velocity fields with time is seen from Fig. 6. The value of the correlation oscillates between positive and negative values indicating the 5 min oscillatory signal which is to a certain extent still present in the data because no filtering in time was possible. The correlation between I_c and v_c are oscillating and negative and higher for the deeper originating line II than for line I. Also the amplitude of fluctuations is smaller for the deeper originating line.

Full width at half maximum

This parameter reflects also non thermal motions being larger in areas with enhanced turbulence. From Fig. 4 it is seen that it is weakly correlated with I_r, the local temperature field. The correlation is positive that means for enhanced I_r values the turbulence is also enhanced. For the correlation of this parameter with line center intensity I_c the situation is not so clear: during the first 6 minutes of the evolution of the field, the correlation is negative, enhanced turbulence occurs at lower intensity values (intergranulum) but then the value decreases.

5. Conclusions

We have shown that it is possible to use 2-D scans in order to study the dynamics of solar granulation by obtaining 2-D spectra. Thus 2 dimensional maps of the line parameters continuum intensity, residual line intensity, full width at half maximum and line center velocity were obtained as a time sequence.

While this technique has some limitations, the data reduction is straightforward. The results are consistent with existing models. However, they also clearly demonstrate the complex nature of granulation. The temporal variation of the correlation can be mainly attributed to the evolutionary effects in the 2-D field observed. Therefore, the variation of the values shows that it does not make sense to speak of correlations between line parameters when studying small areas. The temporal evolution of the parameters is also clearly seen on the error bars. These error bars are influenced by seeing as well however as it is shown in Fig. 5, the influence of seeing on the rms variation of the continuum intensity seems to be small.

As it was pointed out e.g. in Komm et al. (1990), there exists a transition of physical properties of granulation at a height of about 200 km. For line II that originates deeper than line I the correlation values were found to be enhanced which underlines that. The 2-D maps given by Figs. 1 and 2 show some similar structures in the parameters that are seen in all maps of the time series.

This study for the first time demonstrates the influence of evolution on the behavior of the line parameters.

Acknowledgements

A. H. thanks the 'Austrian Fonds zur Förderung der wissenschaftlichen Forschung' for supporting these investigations. A. K. and J. R. acknowledge the grant VEGA 2/3015/23, the German DFG grant Nr. 436 SLK 113/7 and A. H., A. K., J. R. the Austrian and Slovak Academy of Sciences.

The Vacuum Tower Telescope is operated by the Kiepenheuer–Institut für Sonnenphysik, Freiburg, at the Observatorio del Teide of the Instituto de Astrofisica de Canarias.

References

Apslund, M., Nordlund, A., Trampedach, R., Allende Preto, C., Stein, R.F., 2000, A&A 359, 729

Bellot Rubio, L.R., Tritschler, A., Schlichenmaier, R., 2003, Frontiers of High Resolution Spectroscopy, 25th meeting of the IAU, Joint Discussion 20, 23-24 July 2003, Sydney, Australia

Bendlin, C., Volkmer, R., 1995, A&AS, 112, 371

Espagnet, O., Muller, R., Roudier, T., Mein, N., Mein, P., 1995, A&A Suppl., 109, 79

Frutiger, C., Solanki, S.K., Fligge, M., Bruls, J.H.M.J., 2000, A&A, 358, 1109

Gadun, A.S., Hanslmeier, A., Pikalov, K.N., 1997, A&A 320, 1001

Gadun, A.S., Solanki, S.K., Johannesson, A., 1999, A&A 530, 1018

Gadun, A.S., Hanslmeier, A., Kučera, A., Rybák, J., Wöhl, H., 2000, A&A 363, 289

Hanslmeier, A., Mattig, W., Nesis, A., 1990, A&A 238, 354

Hanslmeier, A., Nesis, A., Mattig, W., 1993, A&A 270, 516

Hanslmeier, A., Nesis, A., Mattig, W., 1994, A&A 288, 960

Hanslmeier, A., Kučera, A., Rybák, J., Neunteufel, B., Wöhl H., 2000, A&A 356, 308

Hanslmeier, A., 2003, in: Schielicke, R.E.(ed.): Reviews in Modern Astronomy 16, The Cosmic Circuit of Matter, p. 55 ff. (Wiley-VCH, Weinheim)

Hirzberger, J., Bonet, J.A., Vazquez, M., Hanslmeier, A., 1997, ApJ, 480, 406
Hirzberger, J.; Koschinsky, M.; Kneer, F.; Ritter, C., 2001, A&A 367, 1011
Holweger, H., Kneer, F.J., 1989, in Solar and Stellar Granulation, R.J. Rutten, G. Severino eds., ASI Ser. C 263, 173
Kentischer, T.J., Schmidt, W., Sigwarth, M., Uexküll, M. von, 1998, A&A 340, 569
Komm, R., Mattig, W., Nesis, A., 1990, A&A 239, 340
Komm, R., Mattig W., Nesis, A., 1991a, A&A 243, 251
Komm, R., Mattig W., Nesis, A., 1991b, A&A 252, 812
Koschinsky, M., Kneer, F., Hirzberger, J., 2001, A&A 365, 588
Krat, V.A., 1973, Solar Phys. 32, 307
Krieg, J., Wunnenberg, M., Kneer, F.J., Koschinsky, M., Ritter, C., 1999, A&A, 343, 98
Krieg, J., Kneer, F.J., Koschinsky, M., Ritter, C., 2000, A&A 360, 1157
Kučera, A., Rybák, J., Wöhl, H., 1995, A&A 298, 917
Kučera, A., Balthasar, H., Rybák, J., Wöhl, H., 1998, A&A, 332, 1069
Mattig, W., Schlebbe, H., 1974, Sol. Phys. 34, 299
Lites, B.W., Nordlund, A., Scharmer, G.B., 1989 in Solar and Stellar Granulation, R.J. Rutten, G. Severino eds., ASI Ser. C 263, 349
Muller, R., in Motions in the Solar Atmosphere, A. Hanslmeier, M. Messerotti eds., ASSL, Kluwer, 1999, 35
Nesis, A., Hanslmeier, A., Hammer, R., Komm, R., Mattig, W., Staiger, J., 1992, A&A 253, 561
Nesis, A., Hanslmeier, A., Hammer, R., Komm, R., Mattig, W., Staiger, J., 1993, A&A 279, 599
Nordlund, A., 2003, In: Dynamic Sun. Edited by B. N. Dwivedi. Cambridge (UK): Cambridge University Press, ISBN 0-521-81057-4, 2003, p. 148 - 164
Schröter, E.H., Soltau, D., Wiehr, E., 1985, Vistas in Astronomy, 28, 519
Wiehr, E., Kneer, F.J., 1988, A&A, 195, 310
Wöhl, H., Kučera, A., Rybák, J., Hanslmeier, A., 2002, A&A 394, 1077.